Foams Based on Low Density Polyethylene/ Hectorite Nanocomposites: Thermal Stability and Thermomechanical Properties

J. I. Velasco,[1] M. Antunes,[1] O. Ayyad,[1] C. Saiz-Arroyo,[2] M. A. Rodríguez-Pérez,[2] F. Hidalgo,[3] J. A. de Saja[2]

[1]*Centre Català del Plàstic, Departament de Ciència dels Materials i Enginyeria Metal·lúrgica, Universitat Politècnica de Catalunya, C/ Colom 114, E-08222 Terrassa, Barcelona, Spain*
[2]*Departamento de Física de la Materia Condensada, Cristalografía y Mineralogía, Facultad de Ciencias, Universidad de Valladolid, 47011 Valladolid, Spain*
[3]*Microcel S.A. Polígono de Villalonquejar, Burgos, Spain*

Received 13 September 2006; accepted 26 December 2006
DOI 10.1002/app.26254
Published online 25 April 2007 in Wiley InterScience (www.interscience.wiley.com).

ABSTRACT: Novel polymer nanocomposite foams made by a two step compression molding method are analyzed in this article. Nanocomposites of low density polyethylene and an organo-modified hectorite were first melt compounded and then foamed using a compression molding method. To study the influence of the presence and the amount of hectorite in both mechanical and thermal properties, samples with 3% and 7% content of hectorite were prepared. Polyethylene crystalline characteristics and thermal stability of the samples were studied by differential scanning calorimetry (DSC) and thermogravimetric analysis (TGA), respectively. Mechanical properties of foams and solid nanocomposites were analyzed by using dynamical mechanical analysis (DMA). Thermal expansion of the samples was analyzed by thermomechanical analysis. The results indicate that the exfoliation of hectorite platelets was achieved after the foaming process, but not during the melt mixing step. Foams with hectorite nanoparticles exhibit improved thermal stability and mechanical properties when compared with neat polymeric foams. © 2007 Wiley Periodicals, Inc. J Appl Polym Sci 105: 1658–1667, 2007

Key words: nanocomposites; polyolefin foams; dynamic mechanical analysis; LDPE

INTRODUCTION

Polymer-layered silicate nanocomposites have recently gained a great deal of attention as they offer new possibilities to provide superior properties when compared with pure polymers and conventional filled composites. The properties include high dimensional stability, high heat deflection temperature, reduced gas permeability, improved flame retardancy, and enhanced mechanical properties.[1,2] Polymer foams, on the other hand, are two-phase materials in which a gas is dispersed in a continuous macromolecular phase. These materials are important items in the economy, and, because of technical, commercial, and environmental issues, they represent an interesting dynamic in 21st century society.[3] However, the foam applications are limited by the inferior mechanical strength, poor surface quality, and low thermal and dimensional stability of these materials in comparison with dense solids.

To improve polymer foams properties, several researchers have focused their attention in how to combine the knowledge on foams and polymer nanocomposites.[1] By using a small amount of clay nanoparticles into the polymer matrix it is possible to obtain a significant improvement in a wide variety of properties. Furthermore, the nanometer dimension of nanoclays is especially beneficial for reinforcing foamed materials, considering the thickness of foam cell walls in the micrometer range. Most efforts related with this kind of experiments have been focused in the production of microcellular foams fabricated using a continuous process and studying the influence of the addition of nanoclays into the polymer matrix, both on foaming process and cellular structure.[4–9]

Shen et al.[4] used carbon nanofibers (CNFs) as nucleating agents to produce polystyrene nanocomposite foams. They obtained microcellular foams with uniform cell size distributions and proved that CNFs improved the nucleation efficiency in the foaming process. Lee et al.[5] investigated the effect of clay particles on the cell morphology of HDPE-clay

Correspondence to: M. A. Rodríguez-Pérez (marrod@fmc.uva.es).

Contract grant sponsor: Junta de Castilla y León, Spanish Ministry of Education and Science; contract grant numbers: VA026/03, MAT 2003-06,797.
Contract grant sponsor: FEDER.

nanocomposite foams produced using a batch foaming process using supercritical CO_2. They demonstrated that in comparison with pure HDPE nanocomposites produced it was obtained much finer and more uniform cellular structures. Nam et al.[6] produced polypropylene/clay nanocomposites foamed in an autoclave in a batch process using supercritical CO_2. They studied the correlation between foam structure and rheological properties of the polypropylene clay composites. Mitsunaga et al.[7] successfully prepared intercalated polycarbonate/clay nanocomposites by using the melt intercalation method in the presence of a compatibilizer. After this, they foamed the nanocomposites using supercritical CO_2 as foaming agent. They obtained a significant improvement in most of the material properties. Reverchon et al.[8] and Zeng et al.[9] reviewed the use of supercritical fluids like CO_2 as foaming agent to produce foams from polymer nanocomposites.

On the other hand, interest in polyolefin nanocomposites has emerged due to their promise of improved performance in packaging and engineering applications. Chemical modification of these resins, in particular the grafting of pendant anhydride groups has been used successfully to overcome problems associated with poor phase adhesion in polyolefin/clay systems.[10] Nevertheless, in most cases using the most common methods to produce polymer nanocomposites the fabrication of polyolefin/clay composites leads to intercalated structures instead of the desired exfoliated ones.[5,10,11–17]

As it was previously mentioned, in most studies related with polymer nanocomposite foams, the solid nanocomposites are foamed using a batch foaming process with supercritical CO_2 as foaming agent. In this article, we introduce a commonly used foaming technique such as compression molding[18,19] using dycumil peroxide as crosslinking agent and azodicarbonamide (ADC) as foaming agent, as a tool to produce exfoliated low density polyethylene (LDPE) nanocomposite foams.[20] One of the main targets of this investigation is to gain knowledge on the effects of hectorite nanoparticles on the structure and physical properties of foamed polyethylene.

MATERIALS

Materials and compounding

At first, a low density polyethylene (LDPE), Stamylan LD 2404A (100.00 phr) (density 0,925 g/cm^3 and MFI 4.2 g/10 min at 190°C and 2.16 kg), manufactured by Sabic Europetrochemicals® (Germany), was compounded using a two-roll mill at a constant temperature of 120°C and constant speed of 60 rpm for no more than 5 min with the following materials

a. Azodicarbonamide (ADC, 18.50 phr) used as chemical blowing agent.
b. Dicumyl peroxide (DCP, 1.70 phr) used as crosslinking agent.
c. Stearic acid (0.11 phr) used as a lubricant.
d. Zinc oxide (0.075 phr) used as ADC activator.

An organic derivative of hectorite (Bentone 108, from Elementis Specialties, UK), chemically modified with dimethyl dehydrogenated tallow ammonium chloride (2M2HT), with a density of 1.7 g/cm^3, basal spacing (d_{001}) of 2.5 nm and an average specific area of 700 m^2/g, was used.

Secondly, a masterbatch was prepared by mixing the powdery hectorite and a compatibilizer polymer at 160°C and 160 rpm in a twin-screw extruder (Collin Kneter 25 × 36D). High density polyethylene grafted with maleic anhydride (Fusabond E MB100D, DuPont), with a density of 0.960 g/cm^3 and MFI of 2 g/10 min at 190°C and 2.16 kg was used as compatibilizer.

Finally, two composites were prepared using the hectorite masterbatch and the previously compounded LDPE: the first one (PE3) with a 3 wt % content of hectorite and the second one (PE7) with a 7 wt % content. The extrudates were water-cooled and pelletized.

Foaming process

Precursor materials for foaming were compression-molded in a hot-plate press (IQAP-LAP PL-15). Pellets were initially placed into a mold (3.5 mm deep and 74 mm in diameter) to slightly overfill it and subjected to heating at 110–115°C for 3 min until melting, followed by a final step at the same temperature and applying a constant pressure of 25 bar for 3 min. The resulting discs were cooled under pressure using recirculating water.

A two-step compression molding foaming process was used for all the studied specimens.[18,19] In the first step (prefoaming), the solid discs were placed in the circular mold and heated at temperatures ranging from 123°C to 140°C applying a constant pressure of 40 bar for 90 min. After this time, the pressure was released allowing the foam to partially grow. The expansion ratio in this prefoaming step was fixed in a value around three. The second step (foaming) consisted of the free expansion of the prefoamed samples at a higher temperature, typically between 140°C and 180°C, for no more than 30 min. An expansion ratio of 11 was set for this second step.

EXPERIMENTAL

Density

Density measurements were performed by Archimedes principle using the density determination kit for the AT261 Mettler balance.

Differential scanning calorimetry

Characteristic thermal properties of the materials were studied by means of a Mettler DSC822[e] differential scanning calorimeter, previously calibrated with indium, zinc and *n*-octane. The weights of the samples were 2.5 mg.

To obtain both melting point and crystallinity of the samples the following heating program was chosen:

1st Segment: samples were heated from 30°C to 190°C at a heating rate of 20°C/min under nitrogen atmosphere. To remove the materials thermal history, an isothermal segment, (3 min), was added at the end of this heating segment.

2nd Segment: samples were cooled from 190°C to 30°C at 20°C/min under nitrogen atmosphere.

3rd Segment: after a second isothermal step, (1 min at 30°C), samples were heated a second time at 20°C/min, from 30°C to 190°C also under nitrogen atmosphere.

The melting point was taken at the minimum of the enthalpy-temperature curve. The crystallinity was calculated from the area of the differential scanning calorimetry (DSC) peak, dividing the heat of fusion by the heat of fusion of a 100% crystalline material, (288 J/g for a 100% crystalline polyethylene). In this calculation, a correction was introduced to take into account the real polymer content in each material.

Thermogravimetric analysis

Thermogravimetric analysis was used to determine the effect of addition of clays on the thermal stability of the samples. Tests were performed in a Mettler TGA/SDTA 851[e]. Samples were heated from 50°C to 850°C at a heating rate of 20°C/min in nitrogen atmosphere. Samples mass was 5 mg.

Wide-angle X-ray scattering

Wide-angle X-ray scattering (WAXS) was used to analyze to determine the crystallinity of the materials. A Bruker D8 diffractometer with CuKα radiation, $\lambda = 0{,}154$ nm, 50 kV, and 20 mA was used. Scans were taken from 1° to 30° with a rotation step of 0.05° and a step time of 0.007 s.

Microscopy

Cell morphology was analyzed by using SEM. A JEOL JSM-820 scanning electron microscope was used. Samples were previously prepared by cutting 1 cm^2 specimens and making them conductive by sputtering deposition of a thin layer of gold. Nanocomposite morphology was analyzed using a Hitachi H-800 transmission electron microscope, (TEM) on ultra-microtomed sheets with a typical thickness of 60 nm.

Gel content

Crosslinking degree, (gel content), was measured following the ASTM D2765-90 standard. The procedure was as follows; the extraction was made in 400 mL of xylene at 140°C for 24 h, 300 ± 5 mg of material, (initial weight) were used. The remaining material, (gel) was dried for 1 h at 140°C and weighted. Gel content was calculated by using eq. (1) and corrected by using the polymer content present in each sample.

$$\text{Gel content} = 100 \times \frac{\text{gel weight}}{\text{initial weight}} \quad (1)$$

Dynamical–mechanical analysis

The DMA equipment (Perkin–Elmer DMA7) was calibrated according to the recommended procedures using the manufacture's software. The storage modulus, (E′), loss modulus, (E″), and loss tangent or loss factor, (tanδ), were obtained under compression geometry in a parallel plate measurement system for both prefoamed and foamed samples, while the nonfoamed samples were measured using a three point bending system.

All the experiments were performed at 1 Hz frequency, between −50°C and 110°C at a heating rate of 5°C/min. The applied static strain was 2% and it was chosen a dynamic strain of 0.11%.

For prefoamed and foamed samples test specimens were prepared in a cylindrical shape with a diameter of 8 mm and a thickness of 6 mm, approximately. For nonfoamed samples test specimens were bars of 20 mm width, 3.5 mm height, and 4 mm depth.

At least three experiments were carried out for each sample. For prefoamed and foamed samples tests were carried out in the thickness direction of the discs. For nonfoamed samples tests were performed with the applied force parallel to the thickness direction of the discs.

Thermal mechanical analysis

The experiments were performed in a DMA7 from Perkin–Elmer in the TMA mode. A parallel plate measuring system was used, with a plate diameter of 15 mm. For all the samples, cylindrical tests specimens were prepared with a diameter of 8 mm. The experiments were performed without applied force on the sample to measure the thermal expansion coefficient. The materials were studied between −40°C and 150°C at a heating rate of 5°C/min.

TABLE I
Materials Designation, Density, Expansion Ratio, and Gel Content Results

Material	Density (kg/m^3)	Expansion ratio	Gel content, (%)
Nonfoamed 0% Hectorite = NF0	969.2 ± 22.9	–	–
Nonfoamed 3% Hectorite = NF3	953.2 ± 14.0	–	–
Nonfoamed 7% Hectorite = NF7	990.5 ± 2.2	–	–
Prefoamed 0% Hectorite = PF0	289.5 ± 6.5	3.3	–
Prefoamed 3% Hectorite = PF3	315.2 ± 1.3	3.0	–
Prefoamed 7% Hectorite = PF7	341.2 ± 14.4	2.9	–
Foamed 0% Hectorite = F0	84.0 ± 4.4	11.4	35.3
Foamed 3% Hectorite = F3	86.6 ± 5.0	11.0	31.7
Foamed 7% Hectorite = F7	69.7 ± 3.2	14.2	27.8

For each sample at least three tests were carried out. Tests were performed in the same directions as the ones chosen for DMA experiments.

RESULTS AND DISCUSSION

Density and gel content

Table I summarizes the densities, expansion ratio, and gel content of the materials under study. It can be observed that for the same group of samples, (i.e., nonfoamed, prefoamed, and foamed samples) the density values were similar. The expansion ratio, obtained by dividing the density of nonfoamed samples between the densities of the foamed or prefoamed one, reached a value of three for prefoamed samples and 11 for the foamed ones. The main goal of this article is to compare the physical properties of materials with different contents of hectorite, the density and expansion ratio of materials with different hectorite content were keep constant.

As shown in Table I gel content of the foamed materials was slightly reduced when the hectorite was increased.

Micro-structure

It is well known that one of the targets for a successful polymer nanocomposite is to asses the complete exfoliation of the nanoclay into the polymer matrix. In a previous article[20] it was showed by using WAXS that the melt mixing compounding process used to produce the materials of this investigation was not enough to promote a complete exfoliation of the hectorite particles, only achieved during the prefoaming process. This exfoliation was maintained in the foamed samples.

DSC studies of the samples were carried out to study if the polymer crystallinity changed with the addition of nanoclays. DSC results are summarized in Table II. It can be observed that the crystallinity value (obtained on the first heating, cooling, and second heating segments) is not affected by the presence of hectorite, but it is clearly affected by the prefoaming and foaming steps. In general terms, the nonfoamed material has a higher crystallinity than the prefoamed and foamed materials. This result was also confirmed by the crystallinity values calculated by WAXS, (they are also collected in Table II).

The polymer in the foam, crystallizes in exceptional conditions, that is in the presence of a gas and in very thin walls, (these walls are usually thinner than 2 μm, which is smaller than the typical dimensions of the spherulites in a LDPE solid sheet), which has been stretched and crosslinked during foaming. Therefore, it should be expected that the solid polymer in the cell walls could have a different morphology and consequently different properties. Almanza et al.[21] and Rodriguez-Perez et al.[22] have studied this fact for LDPE foams produced by a nitrogen solution process, showing similar trends to those observed in the materials of this article.

The results for melting and crystallization temperatures are also collected in Table II. Differences between composites with different hectorite content and kind of sample are very small. Thus, there are no clear trends for these properties, which seem to be independent on the hectorite content and foaming steps.

TABLE II
DSC Results

	1st Segment		2nd Segment		3rd Segment		
Sample	X_c (%)	T_m (°C)	X_c (%)	T_c (°C)	X_c (%)	T_m (°C)	X_c (%) WAXS
NF0	38.2	113.0	38.8	96.6	36.0	111.7	47.4
PF0	33.9	112.3	35.7	96.0	34.4	111.4	36.7
F0	32.0	110.0	35.1	95.0	32.8	110.4	37.4
NF3	35.5	113.1	36.8	96.6	33.5	111.3	49.0
PF3	33.1	112.0	35.4	96.0	33.8	110.7	38.3
F3	28.7	109.6	31.2	94.8	29.4	110.5	37.0
NF7	36.3	112.0	38.3	95.6	35.9	110.4	45.9
PF7	36.1	111.7	37.1	95.6	35.2	111.1	37.1
F7	29.3	109.8	32.8	94.2	30.9	110.5	37.1

T_m, melting temperature; X_c, crystallinity; T_c crystallization temperature.

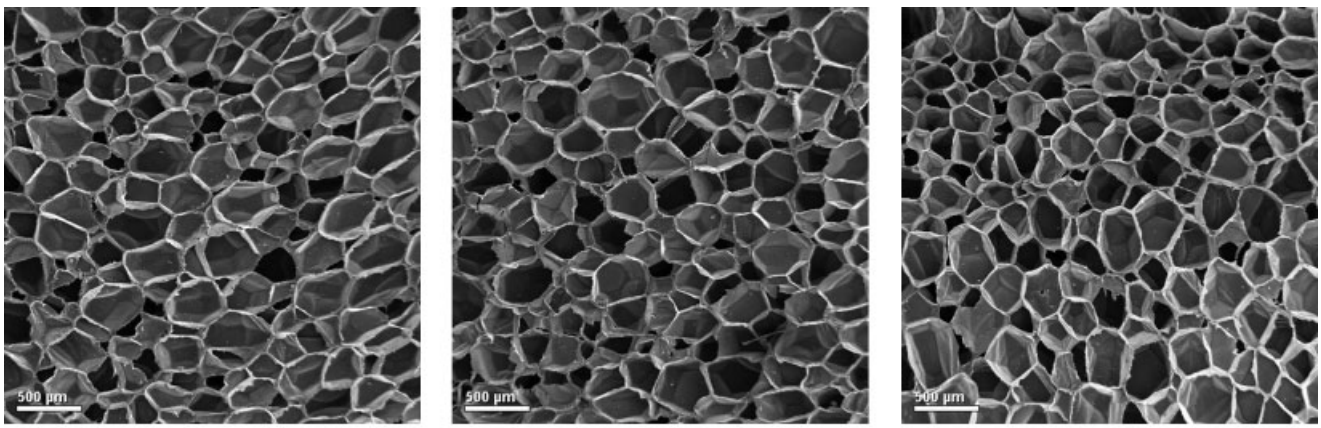

Figure 1 Micrographs of foamed samples: (a) PE0, (b) PE3, (c) PE7.

Other important aspect that has to be considered when foamed materials are analyzed is the cellular structure. Micrographs of foamed samples can be seen in Figure 1(a–c). A closed cell cellular structure characterized all the produced materials. Cell size was $\sim$ 200 μm for all the studied foams. No significant differences in the cellular structure of samples with and without hectorite were found. Therefore, it has been concluded that hectorite nanoparticles did not play role as nucleating agents in the foaming behavior of these materials.[20]

Figure 2 shows a typical TEM picture of a foamed sample. The nanocomposite consisted of mixed dispersed individual hectorite and stacks of hectorite platelets. Foaming agent decomposition residues were also present in the form of regular particles of typical size 50 nm.

Thermal behavior

Thermogravimetric analysis

Thermograms corresponding to foamed samples are presented in Figure 3. Results corresponding to weight loss on each step and residues content are collected in Table III.

First and second steps in all the thermograms can be associated with the decomposition of foaming agent, additives, and residues of foaming agent. Third step is associated to the decomposition of the polymer matrix. Weight loss on each step for all the samples does not show significant differences (Table III). The used nanoclay, is organically modified, so approximately only the half hectorite content will appear in the residues, (the organic part decomposes during the experiment). The amount of residues increased as hectorite content increased. In this sense, if we take into account the amount of residues of samples without hectorite and subtract it from the amount of residues of samples with hectorite, the result is in agreement with the amount of hectorite that should remain after the decomposition of the organic part of the nanoparticle.

Generally, the incorporation of clay into the polymer matrix has been found to enhance thermal stability by acting as a superior insulator and mass transport barrier to the volatile products generated during decomposition.[2] The clay acts as a heat barrier, which enhances the overall thermal stability of the system, as well as assist in the formation of char after thermal decomposition. In the early stages of thermal decompositions the clay would shift the decomposition to higher temperature. Thermogravimetric studies of the samples were carried out to study if the previous effects showed in our materials.

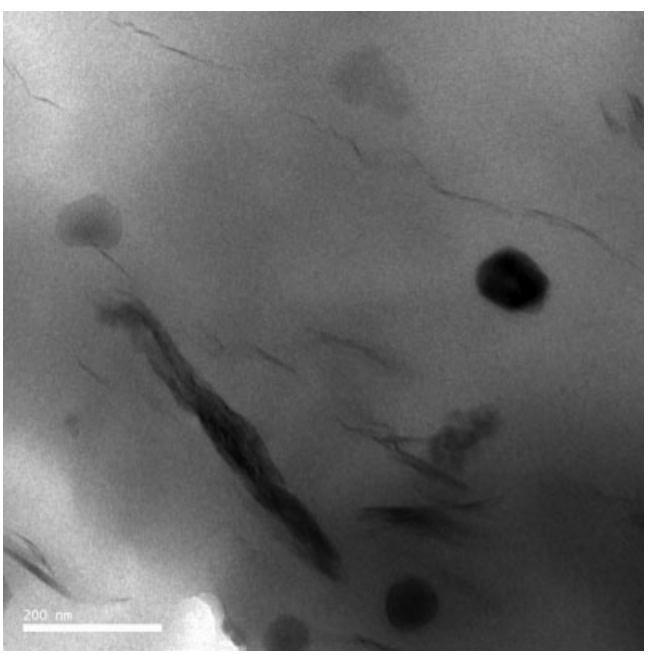

Figure 2 Typical TEM image for a foamed composite.

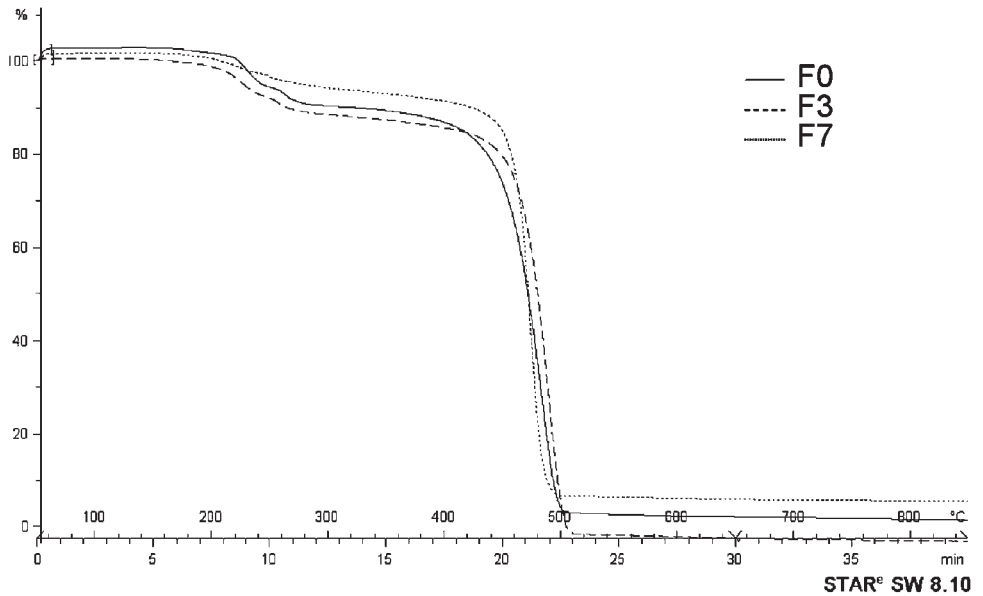

Figure 3 Thermograms of foamed samples.

It can be observed that the addition of nanoclays combined with the foaming improves thermal stability of the samples (an increase of 8°C was detected) (Fig. 3). In the case of solid materials and prefoamed materials this improvement is not so clear in the experimental data (improvement of 3°C for solid materials and no improvement for prefoamed materials). It has been previously explained that the best exfoliation is obtained after foaming the materials, this could be one of the reasons that justify why after foaming the thermal stability was improved in a higher extend.

Dynamic mechanical analysis

The experimental results corresponding to DMA tests of foamed and nonfoamed samples are shown in Figures 4 and 5. The storage modulus, (E′) and loss factor, (tanδ), are plotted as a function of temperature.

For both kinds of materials, it can be observed how all the curves present the typical DMA behavior of LDPE with the presence of β and α relaxations. The presence of hectorite can be detected in the storage modulus curve for both nonfoamed and foamed samples. As it can be observed, storage modulus increases as the hectorite weight content increases. This difference is more evident for the material with 7% weight content.

To partially eliminate the density differences between samples, the reduced specific storage modulus (i.e., storage modulus divided by the density of each sample) obtained at room temperature, was calculated. The value for the material without nanofiller was 3.5×10^4 Nm/kg, this value increased to a value of 1.5×10^5 for the material with a 7% filler content. Therefore, for foamed samples, mechanical properties of the material are clearly improved with the addition of 7% of nanoclays.

Relaxations of LDPE have been widely studied. At low temperatures, (around −20°C), β relaxation

TABLE III
TGA Results

	1st Step		2nd Step		3rd Step			
Sample	% w.1.	T (°C)	% w.1.	T (°C)	% w.1.	T (°C)	% Residues	T_{onset} (°C)
NF0	9.02	228.4	5.29	239.9	85.97	489.5	0.94	460.21
PF0	8.95	230.3	4.14	240.3	86.67	489.8	0.97	460.25
F0	7.08	232.3	4.84	240.4	88.72	486.4	1.26	456.50
NF3	8.02	229.3	3.79	239.8	87.45	475.1	2.28	462.08
PF3	7.14	229.9	3.18	259.9	88.95	474.1	2.02	459.84
F3	5.95	230.9	4.09	260.4	91.71	482.2	2.70	461.61
NF7	7.70	227.3	2.84	239.7	86.65	467.6	3.76	463.13
PF7	7.27	223.1	3.09	256.5	87.29	467.8	4.37	460.24
F7	4.18	227.3	2.44	254.1	89.07	477.7	5.13	464.67

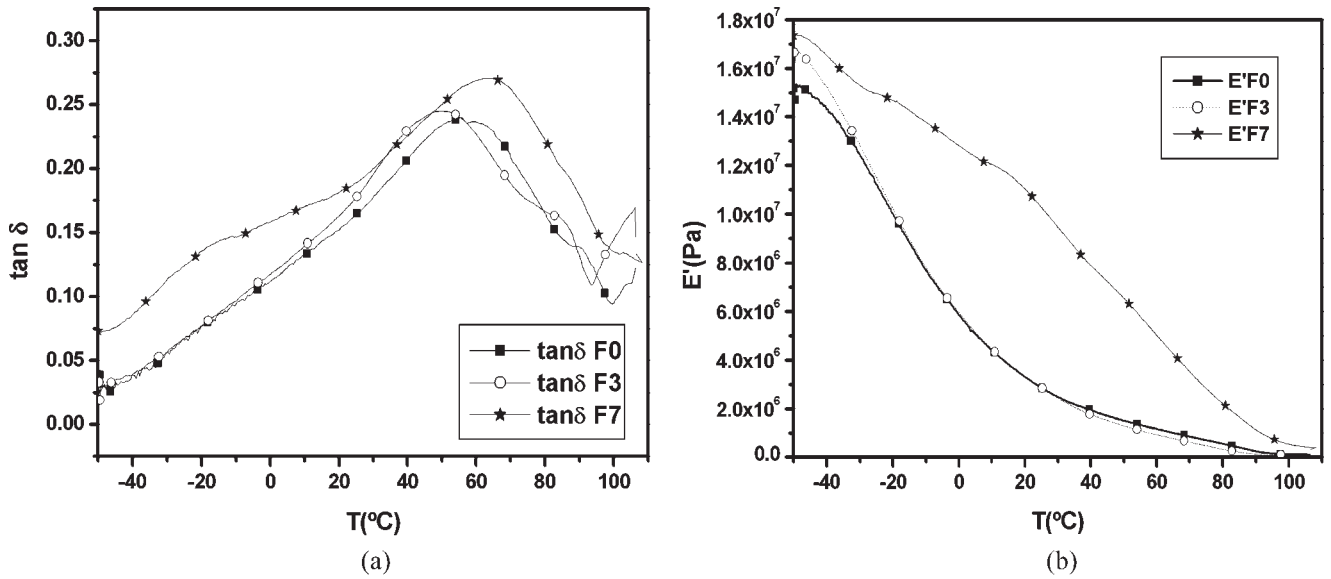

Figure 4 (a) Tanδ versus temperature for foamed samples, and (b) storage modulus versus temperature for foamed samples.

appears, and can be detected as a shoulder in the tanδ curve or as a peak in the loss modulus curve. In nonfoamed polyethylene, this relaxation results from motions of chain units located in the interfacial region and its existence is not universal in the different types of polyethylene, being conditioned by the presence of an interfacial content higher than about 7%. The α relaxation can be seen at higher temperatures, (between 30°C and 120°C).[23] It can be detected as a wide peak in the tanδ curve or a shoulder in the loss modulus curve. The α relaxation has been associated with the crystalline part of the polymer. In fact the position of the relaxation is controlled by the thickness of the lamellae.[23]

In the obtained DMA results α and β relaxations can be observed in the above described way for all the studied samples. In Table IV the temperatures at which α and β relaxations appear are summarized. It can be observed how β relaxation appears at higher temperatures for foamed samples than for nonfoamed samples and prefoamed samples. α-Relaxation appears at lower temperatures for foamed samples than for the other studied samples. The hectorite content seems not to have a significant effect on the shifting and intensity of the relaxations.

It was previously mentioned, that crystallinity values were affected by foaming process and not by hectorite content. Therefore one possible explanation

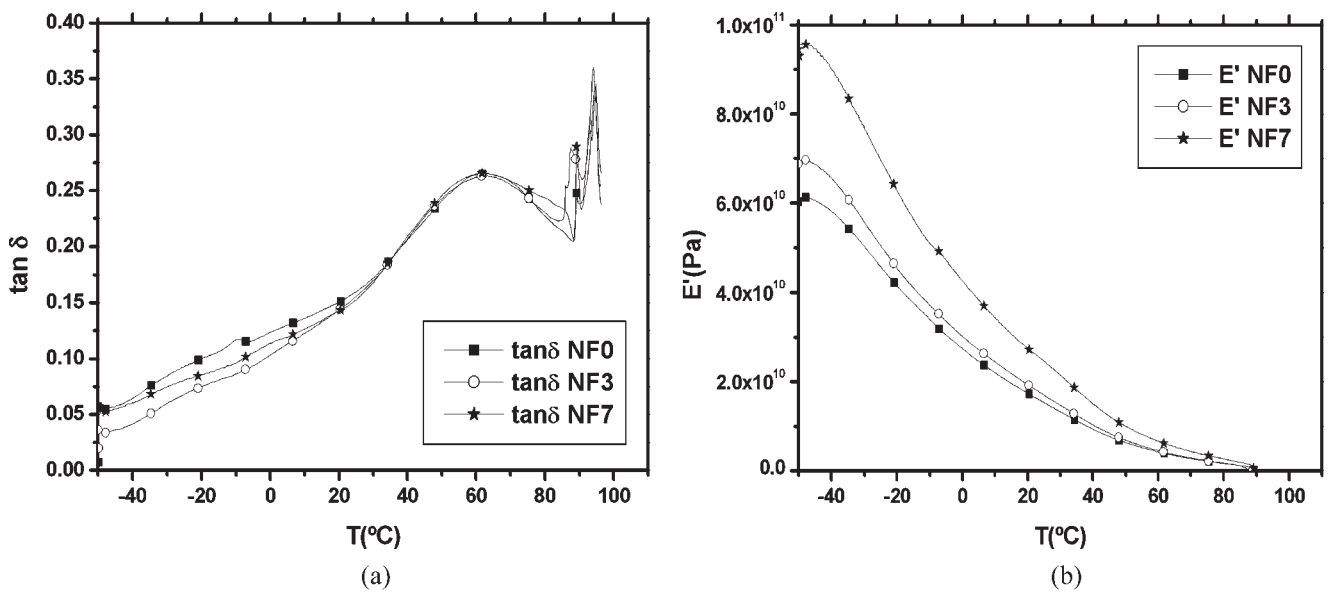

Figure 5 (a) Tanδ versus temperature for nonfoamed samples, and (b) storage modulus versus temperature for nonfoamed samples.

TABLE IV
Temperature and Intensity of α and β Relaxations Detected in the Tanδ Curve

Sample	T_β (°C)	tanδ (β)	T_α (°C)	tanδ (α)
F0	−20.44	0.074	55.41	0.23
F3	−19.83	0.077	49.67	0.24
F7	−17.04	0.140	63.39	0.27
PF0	−20.12	0.048	65.63	0.24
PF3	−20.64	0.054	64.23	0.21
PF7	−20.71	0.078	64.23	0.22
NF0	−28.15	0.088	62.52	0.26
NF3	−26.23	0.066	63.26	0.26
NF7	−29.99	0.074	62.02	0.26

of the relaxation shifting would be related with the different polymer morphology of the different materials. To prove if the thickness of the lamellae for foamed samples was smaller than that of nonfoamed samples, the thickness of lamellae for both kinds of samples were calculated using the model given by Alberola et al. using the DSC data.[24] In Figure 6(a–c), the distribution of lamellae thickness is presented for nonfoamed and foamed samples with different hectorite content. It can be observed that in all cases lamellae thickness is larger for nonfoamed samples than for foamed samples. This should be the reason of the displacement of α-relaxation to higher temperatures for nonfoamed samples.

On the other hand, foamed samples are the ones with lower crystallinity value and consequently with higher interfacial content between crystalline and amorphous phase, which would explain that β relaxation is displaced to higher temperatures for these materials, and particularly for F7 sample in which

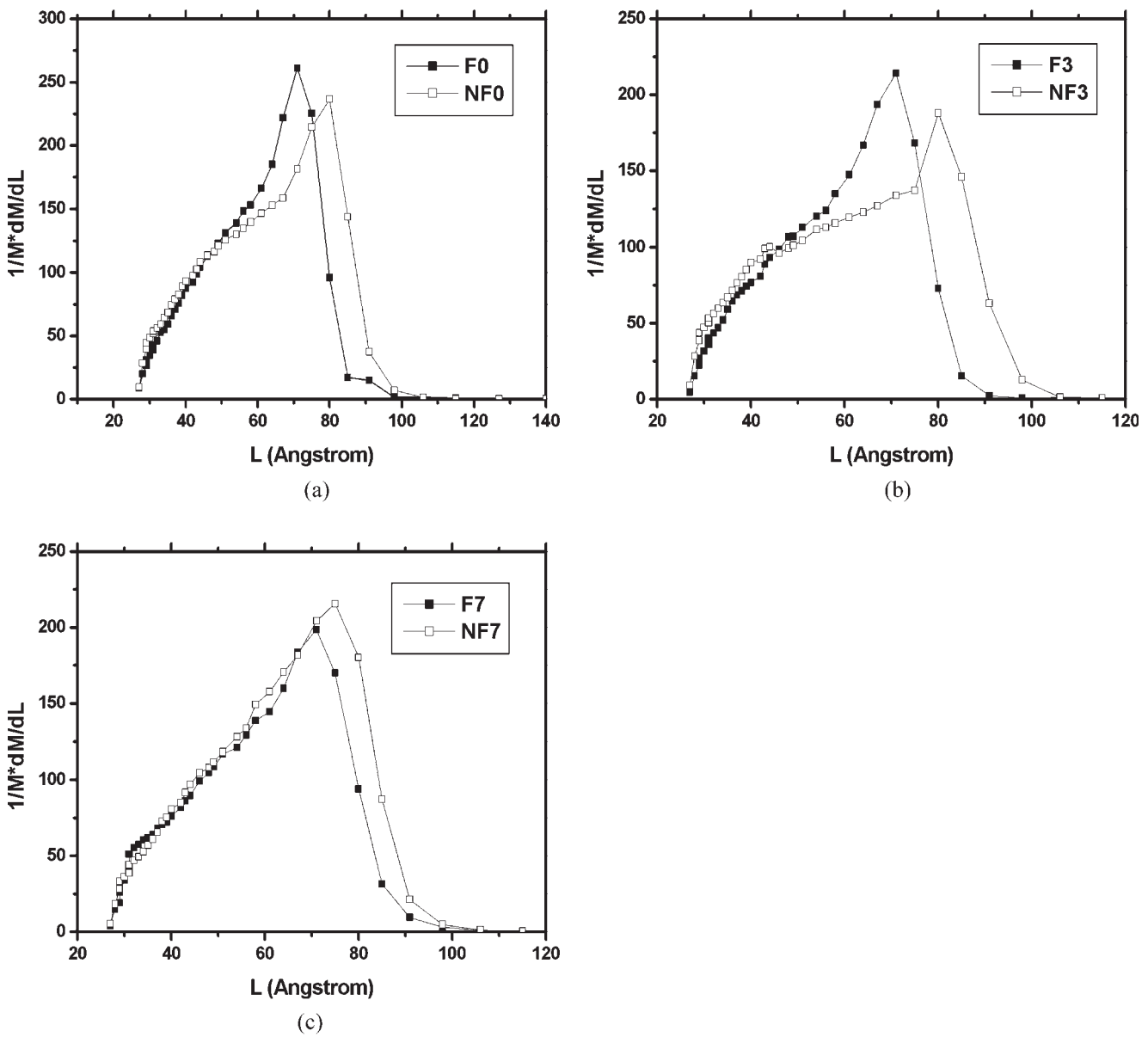

Figure 6 Distribution of lamellar thickness for both nonfoamed and foamed samples.

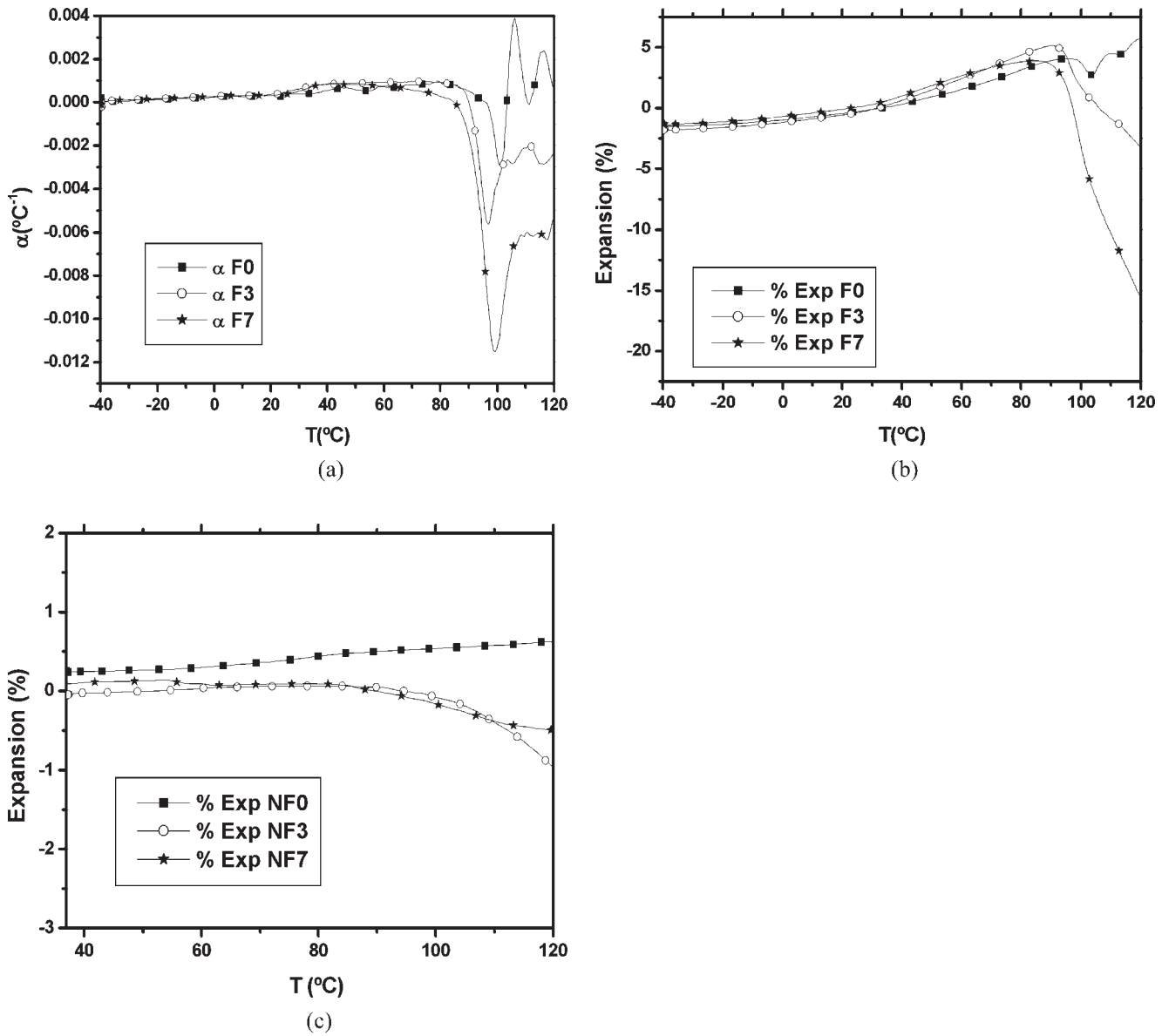

Figure 7 (a) Linear thermal expansion coefficient of foamed samples versus temperature, (b) percentage of expansion of foamed samples versus temperature, and (c) percentage of volumetric expansion of nonfoamed samples versus temperature.

the hectorite nanoparticle/polyethylene interface would be affecting.

Thermomechanical analysis

It is known that the addition of fillers or reinforcing agents into plastics mitigates to some degree the high thermal expansion of these materials by two different mechanisms: (a) volume dilution with a material of lower coefficient of thermal expansion, and (b) mechanical constraint by a dispersed phase with low coefficient of thermal expansion and higher modulus.

Polymer nanocomposites made by exfoliating the typical 1 nm thick aluminosilicate platelets of the clay-mineral, offer exciting possibilities for resolving the problem of the high thermal expansion coefficient that polymers posses. These nanoclays platelets have a high modulus and high aspect ratios for effective reinforcement and mechanical restraint of thermal expansion.[25]

The percentage of material expansion was calculated as follows:

$$\frac{l_i - l_0}{l_0} \times 100 \qquad (2)$$

where l_0 is the initial height of the sample and l_i is the height of the sample at a temperature T_i.

In Figure 7(a) linear thermal expansion coefficient corresponding to foamed samples is represented as a function of temperature, and in Figure 7(b) the per-

centage of material expansion is represented also as a function of temperature for the same kind of materials. It can be observed that there are no significant differences in the behavior of the samples with and without hectorite. The percentage of expansion for the foamed samples is almost the same in all cases. Therefore, the expected reduction of thermal expansion was not found in the foamed materials. The percentage of volumetric expansion of nonfoamed samples is represented as a function of temperature in Figure 7(c). As it was expected for the solid nanocomposites the presence of hectorite reduces the expansion of the material. However, this effect is not observed in the foamed materials.

Previous articles[26,27] on the thermal expansion of closed cell polyolefin based foams have showed that in addition to the contribution of the thermal expansion of the polymeric matrix there is an additional effect related with the expansion of the gas when the temperature increases. Therefore, the expected differences for the foams due to the polymer constraint by the hectorite platelets seem to be compensated in the samples under study by the expansion effect of the gas in the foamed materials.

CONCLUSIONS

As it has been established with this study the compression molding method can be an interesting tool in the production of polyolefin nanocomposite foams. From a practical point of view, with the procedure carried-out; there is no need for a complete exfoliation of the nanoclay in the compounding step. The exfoliation will occur during foaming.

Both thermal and mechanical properties of LDPE foams were improved because of the hectorite nanoplatelets. Thermal stability of the samples was enhanced for foamed samples; this is, when the exfoliation of the nanoclay is complete. On the other hand, mechanical properties were improved in both cases, when the nanoclay is intercalated, (nonfoamed samples) and when the nanoclay is exfoliated, (foamed samples). This effect was especially significant for the foamed sample with a 7% content of nanoclay. It was proved that crystallinity degree of the samples was not affected by the presence of hectorite but it was affected by the foaming process because of the different crystallization conditions of the polymer in the foams and in the solid nanocomposites. The different polymer morphology in the foamed materials also affected the position of the relaxations detected in the DMA tests.

References

1. Lee, J. L.; Zeng, C.; Cao, X.; Han, X.; Shen, J.; Xu, G. Compos Sci Technol 2005, 65, 2344.
2. Ray, S. S.; Okamoto, M. Prog Polym Sci 2003, 28, 1539.
3. Rodríguez-Pérez, M. A. Adv Polym Sci 2005, 184, 97.
4. Shen, J.; Zeng, C.; Lee, L. J. Polymer 2005, 46, 5218.
5. Lee, Y. H.; Park, C. B.; Wang, K. H. J Cell Plast 2005, 41, 487.
6. Nam, P. H.; Maiti, P.; Okamoto, M.; Kotaka, T.; Hasegawa, N.; Usuki, A. Polym Eng Sci 2002, 42, 1907.
7. Mitsunaga, M.; Ito, Y.; Ray, S. S.; Okamoto, M.; Hironaka, K. Macromol Mater Eng 2003, 288, 543.
8. Reverchon, E.; Volpe, M. C.; Caputo, G. Curr Opin Solid State Mater Sci 2003, 7, 391.
9. Zeng, C.; Ha, X.; Lee, L. J.; Koeling, K. W.; Tomasko, D. L. Adv Mater 2003, 20, 1743.
10. Gopakumar, T. G.; Lee, J. A.; Kontopoulou, M. Polymer 2002, 43, 5483.
11. Morawiec, J.; Pawlak, A.; Slouf, M.; Galeski, A.; Piorkowska, E.; Krasnikowa, N. Eur Polym J 2005, 41, 1115.
12. Zanetti, M.; Bracco, P.; Costa, L. Polym Degrad Stabil 2004, 85, 657.
13. Wang, K. H.; Choi, M. H.; Koo, C. M.; Xu, M.; Chung, I. J.; Jong, M. C.; Choi, S. W.; Song, H. H. J Polym Sci Part B: Polym Phys 2002, 40, 1454.
14. Alexandre, M.; Dubois, P.; Sun, T.; Garres, J. M.; Jérôme, R. Polymer 2002, 43, 2123.
15. Wang, K. H.; Choi, M. H.; Koo, C. M.; Choi, Y. S.; Chung, I. J. Polymer 2001, 42, 9819.
16. Kato, M.; Okamoto, H.; Hasegawa, N.; Tsukigase, A.; Usuki, A. Polym Eng Sci 2003, 43, 1312.
17. Liang, G.; Xu, J.; Bao, S.; Xu, W. J Appl Polym Sci 2004, 91, 3974.
18. Park, C. P. Handbook of Polymeric Foams; Klempner, D., Frisch, C., Eds.; Hanser Publishers: New York, 1991.
19. Puri, R. R.; Collington, K. T. Cell Polym 1988, 7, 219.
20. Velasco, J. I.; Antunes, M.; Ayyad, O.; López-Cuesta, J. M.; Gaudon, P.; Saiz-Arroyo, C.; Rodríguez-Pérez, M. A.; De Saja, J. A. Polymer, to appear.
21. Almanza, O.; Rodríguez-Pérez, M. A.; de Saja, J. A. Polymer 2001, 42, 7117.
22. Rodríguez-Pérez, M. A.; de Saja, J. A. J Macromol Sci Phys 2002, 41, 761.
23. Popli, P.; Glotin, M.; Mandelkern, L.; Benson, R. S. J Polym Sci Part B: Polym Phys 1984, 22, 407.
24. Alberola, N.; Cavaille, J. Y.; Pérez, J. J Polym Sci Part B: Polym Phys 1990, 28, 569.
25. Lee, H.; Fasulo, P. D.; Rodgers, W. R.; Paul, D. R. Polymer 2006, 47, 3528.
26. Rodríguez-Pérez, M. A.; Alonso, O.; Duijsens, A.; de Saja, J. A. J Polym Sci Part B: Polym Phys 1988, 36, 2587.
27. Almanza, O. A.; Masso-Moreu, Y.; Mills, N. J.; Rodríguez-Pérez, M. A. J Polym Sci Part B: Polym Phys 2004, 42, 3741.